Analytical Approach to the Short-range Wakefield between Two Conducting Plates Generated by a Sub-relativistic Beam Bunch

Haipeng Wang*

Center for Accelerator Physics
Brookhaven National Lab
Building 901A, Upton, NY11973

Abstract

The muon cooling channel design requires a full space charge and wakefield effects included in the beam dynamic simulation. The worst problem may happen when the sub-relativistic ($\beta=v/c<1$) muon beam bunch is inside of RF cavities. To understand the short-range wakefield and crosscheck with MAFIA simulation, an analytical approach by image charge algorithm has been developed for the geometry of two parallel planner conductors. This paper gives all details of physics and mathematics in the electromagnetic field generation, propagation, reflection and causality issue. The calculated wakefield results have an excellent agreement with MAFIA simulation within a broad range of β [5].

1. Introduction

Current muon ionization cooling design for a muon collider or a neutrino factory requires a full space charge and wakefield effects included in the beam dynamic simulation. The worst problem may exist when the sub-relativistic muon beam bunch ($\beta=v/c<1$) is inside of RF acceleration cavities. The baseline design for the cavity shape is to close the cavity irises by the low Z (which gives less muon scattering) metal conductors (which gives higher shunt impedance). The choice is either the beryllium foil window type [1] or the thin tubes grill type [2]. Whichever is closed to a pillbox type cavity. The transverse space-charge force of the dense beam may reduce the cooling effect. The wakefield may also act on the bunch tail itself. However, this effect has not implemented in the ICOOL [3] simulation yet, because there was a fundamental problem has to solve. That is how to calculate the Coulomb field and wakefield when the sub-relativistic beam bunch is still inside of RF cavity. MAFIA codes [4] are able to do the job, but exports only believe the wakefield calculation for the ultra-relativistic beam ($\beta=1$) and in the long-range when the beam bunch already left the cavity. There is no any analytical tool suitable to crosscheck the MAFIA simulation in short-range for the sub-relativistic beam [5]. Under this motivation, we found the image charge algorithm is very simple in mathematics and very clear in physics and is a very powerful and interesting tool. The short-range wakefield is dominated by the path length of first a few reflected waves within the cavity. Current 805 MHz beryllium window cavity has a gap distance 7.821cm and a radius 14.28cm, so the short-range waves only depend on the gap distance and reflect between two planner walls. It is a perfect example for exploring the short-range wakefield problem. This development is based on the geometry of two parallel plane conductors and the foundation works of Chao [6][7], Carron [8] and Maresca [9].

2. Sub-relativistic Waves in One-plane Model

Electromagnetic fields generated by a sub-relativistic point charge moving out from an infinite large, planar and perfect-conducting plane can be deduced from Carron's note [8] in cylindrical (r,ϕ, z) coordinates:

* email address: haipeng@bnl.gov

$$e_r = \frac{q}{4\pi\varepsilon_0}\left\{\frac{1}{\gamma^2}\left[\frac{r}{s_-^{\,3}} - \frac{r}{s_+^{\,3}}\right]u(ct-\Re) + \frac{2\beta rz}{\Re(\Re^2-\beta^2 z^2)}\delta(ct-\Re)\right\} \tag{1}$$

$$e_z = \frac{q}{4\pi\varepsilon_0}\left\{\frac{1}{\gamma^2}\left[\frac{z-\beta ct}{s_-^{\,3}} - \frac{z+\beta ct}{s_+^{\,3}}\right]u(ct-\Re) - \frac{2\beta r^2}{\Re(\Re^2-\beta^2 z^2)}\delta(ct-\Re)\right\} \tag{2}$$

$$b_\phi = \frac{q}{4\pi\varepsilon_0 c}\left\{\frac{\beta}{\gamma^2}\left[\frac{r}{s_-^{\,3}} + \frac{r}{s_+^{\,3}}\right]u(ct-\Re) + \frac{2\beta r}{\Re^2-\beta^2 z^2}\delta(ct-\Re)\right\} \tag{3}$$

Here

$$s_- \equiv \sqrt{(\beta ct - z)^2 + r^2/\gamma^2} \tag{4}$$

$$s_+ \equiv \sqrt{(\beta ct + z)^2 + r^2/\gamma^2} \tag{5}$$

And

$$\Re \equiv \sqrt{r^2 + z^2} \tag{6}$$

The positive source particle moves on z-axis and out of conducting surface at z=0, with a relative velocity of $\beta = v/c$, c is the speed of light. $\gamma = 1/\sqrt{1-\beta^2}$.

All fields are independent in azimuth ϕ. Each field component consists of three terms. The terms with the Heaviside step function u(ct-$\Re$) represent Coulomb fields generated by a positive source charge and a negative image charge. Two charges are moving in opposite direction relative to the mirror plane. The third term with the Delta function δ(ct-$\Re$) represents the radiation field. We note that the radiation field only rides on the spherical wavefront, and the Coulomb field resides between the conducting plane and the wavefront. The wavefront originates at (r, z)=(0, 0), with the radius of ct, and expends homogeneously in the speed of light c. The charge particle moves in the velocity of βc, behind the radiation wavefront. Coulomb field surrounds the source particle and propagates with it, but its scope expends with the radiation wavefront. We call the electromagnetic field in term of Coulomb and radiation. Because the Coulomb field has the character of field strength e (or b) $\propto 1/L^2$. The L is the distance between the source and the field point interested. The radiation field has e (or b) $\propto 1/L$. As the particle approaches in relativistic (β=1), the Coulomb field vanishes and only the radiation field left. The charge particle is just riding on the wavefront. In opposite, as the particle stays in static (β=0), the radiation and magnetic fields disappear. Only Coulomb field left, is in the form we knew.

In principle, a charge particle could not move out or move in a perfect conductor due to the image charge effect. In other words, the image current in the conducting plate is infinite high when the source charge is touching the plane. There is a repelling force to prevent the source particle moving to the interception point. In reality, the conductivity of the conducting plate is always finite. Also the source particle moves with a finite energy. If the conducting plate is a thin wall, an energized particle can always pass through the conductor plane. In the mathematics, the image charge method always assumes the electric mirror is a perfect conductor plane. There is a singularity at the interception points. We can avoid this problem by excluding these points in the field integration.

3. Sub-relativistic Waves in Two-plane Model

We now consider a point source charge moving between two conducting planes. Before the radiation wavefront reaches the second conductor plane, there is no new physics from the one-plane model. The information from the second plane has not received yet. After the wavefront strikes the second conductor plane, a new two-plane model need to develop. There are three additional terms (physics points) to add into Carron's field expression (1)-(3).

1) A backward radiation when the source charge exiting out to the second plane.

2) A reflected wave first bounces back from the second conductor plate. As the spherical waves propagated, multiple refection waves will be superimposed. The reflected waves can be represented by the infinite numbers of image charges generated fields originated at different locations. Illustrated in Fig. 1, we can use $z+2ig$ to replace the z in Eqs. (4)-(6) to represent the reflected Coulomb and forward radiation fields. Use $z-g-2ig$ to replace the z in Eq. (6) to represent the reflected backward radiation fields. Here i=0, -1, +1, -2, +2…. The forward means the primary radiation wavefront is in +z direction. The reflected waves can be either +z or –z direction. For example, the first reflected forward radiation is in –z direction, and second reflected forward radiation is in +z direction. The sequence of terms in i=0, -1, +1, -2, +2… also represents the wave front appearance sequence between the two conducting planes. For example, i=0 is a primary wave. i=-1 is first reflected wave, and i=+1 is second reflected wave. These wavefronts are generated at same time but originated at different z positions. The separation of these origins is $2g$. According to the new modifications, the s_- and s_+ become to s_{i-} and s_{i+}, the $\Re$ becomes $\Re_{i+}$ and $\Re_{i-}$.

3) There is no Coulomb field emitted after the source particle left the second plane. So there is a disappearance term attached to the Coulomb field expression.

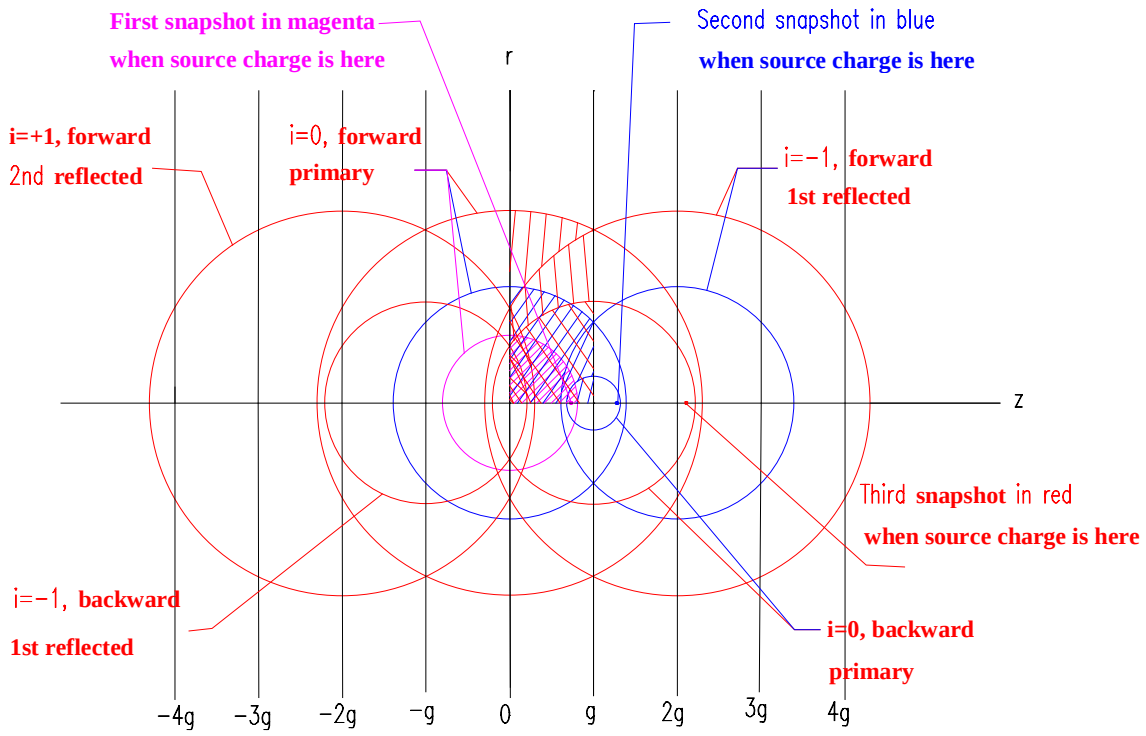

Figure 1: Electromagnetic waves generated by a sub-relativistic charge moving through two conducting plates. The wavefront pictures are taken at three different snapshots (in colors: first, magenta; second, blue; third, red).

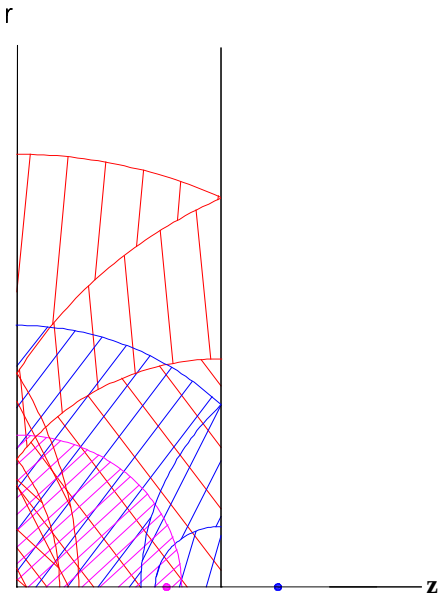

Figure 2: Blow-up view of Fig.1 between two conducting plates.

Now the field expression can be written as in Eqs. (7)-(9).

$$e_r = \frac{q}{4\pi\varepsilon_0}\sum_{i=-\infty}^{+\infty}\left\{\begin{aligned}&\frac{1}{\gamma^2}\left(\frac{r}{s_{i-}^{\ 3}}-\frac{r}{s_{i+}^{\ 3}}\right)u(ct-\Re_{i+})u(\Re_{0-}-ct+\frac{g}{\beta})\\&+\frac{2\beta r(z+2ig)}{\Re_{i+}[\Re_{i+}^{\ 2}-\beta^2(z+2ig)^2]}\delta(ct-\Re_{i+})\\&-\frac{2\beta r(z-g-2ig)}{\Re_{i-}[\Re_{i-}^{\ 2}-\beta^2(z-g-2ig)^2]}\delta(ct-\frac{g}{\beta}-\Re_{i-})\end{aligned}\right\} \tag{7}$$

$$e_z = \frac{q}{4\pi\varepsilon_0}\sum_{i=-\infty}^{+\infty}\left\{\begin{aligned}&\frac{1}{\gamma^2}\left(\frac{z+2ig-\beta ct}{s_{i-}^{\ 3}}-\frac{z+2ig+\beta ct}{s_{i+}^{\ 3}}\right)u(ct-\Re_{i+})u(\Re_{0-}-ct+\frac{g}{\beta})\\&-\frac{2\beta r^2}{\Re_{i+}[\Re_{i+}^{\ 2}-\beta^2(z+2ig)^2]}\delta(ct-\Re_{i+})\\&+\frac{2\beta r^2}{\Re_{i-}[\Re_{i-}^{\ 2}-\beta^2(z-g-2ig)^2]}\delta(ct-\frac{g}{\beta}-\Re_{i-})\end{aligned}\right\} \tag{8}$$

$$b_\phi = \frac{q}{4\pi\varepsilon_0 c}\sum_{i=-\infty}^{+\infty}\left\{\begin{array}{l}\dfrac{\beta}{\gamma^2}\left(\dfrac{r}{{s_{i-}}^3}+\dfrac{r}{{s_{i+}}^3}\right)u(ct-\Re_{i+})u(\Re_{0-}-ct+\dfrac{g}{\beta}) \\ +\dfrac{2\beta r}{{\Re_{i+}}^2-\beta^2(z+2ig)^2}\delta(ct-\Re_{i+}) \\ -\dfrac{2\beta r}{{\Re_{i-}}^2-\beta^2(z-g-2ig)^2}\delta(ct-\dfrac{g}{\beta}-\Re_{i-})\end{array}\right\} \tag{9}$$

Here g is the distance between the two conducting planes.

$$s_{i-} \equiv \sqrt{(\beta ct - z - 2ig)^2 + r^2/\gamma^2} \tag{10}$$

$$s_{i+} \equiv \sqrt{(\beta ct + z + 2ig)^2 + r^2/\gamma^2} \tag{11}$$

$$\Re_{i+} \equiv \sqrt{r^2 + (z+2ig)^2} \tag{12}$$

$$\Re_{i-} \equiv \sqrt{r^2 + (z-2ig-g)^2} \tag{13}$$

Now we want to use the normalized parameters and define:

$$E_r \equiv \frac{4\pi\varepsilon_0 g^2}{q}e_r \qquad E_z \equiv \frac{4\pi\varepsilon_0 g^2}{q}e_z \qquad B_\phi \equiv \frac{4\pi\varepsilon_0 g^2 c}{q}b_\phi \tag{14}$$

$$R \equiv \frac{r}{g} \quad Z \equiv \frac{z}{g} \quad cT \equiv \frac{ct}{g} \tag{15}$$

$$R_{i+} \equiv \frac{\Re_{i+}}{g} = \sqrt{R^2 + (Z+2i)^2} \qquad R_{i-} \equiv \frac{\Re_{i-}}{g} = \sqrt{R^2 + (Z-2i-1)^2} \tag{16}$$

$$S_{i-} \equiv \gamma\frac{s_{i-}}{g} = \sqrt{R^2 + \gamma^2(\beta cT - Z - 2i)^2} \quad S_{i+} \equiv \gamma\frac{s_{i+}}{g} = \sqrt{R^2 + \gamma^2(\beta cT + Z + 2i)^2} \tag{17}$$

Use the relationship:

$${R_{i+}}^2 - \beta^2(Z+2i)^2 = R^2 + (Z+2i)^2/\gamma^2 \tag{18}$$

$${R_{i-}}^2 - \beta^2(Z-2i-1)^2 = R^2 + (Z-2i-1)^2/\gamma^2 \tag{19}$$

Substituting (14)-(19) in equation (7)-(9), we obtain

$$E_r = \sum_{i=-\infty}^{\infty} \left\{ \begin{array}{l} \underbrace{\gamma\left(\frac{R}{S_{i-}^{\ 3}} - \frac{R}{S_{i+}^{\ 3}}\right)\overbrace{u(cT-R_{i+})}^{\text{Appearance Term}}\overbrace{u(R_{0-}-cT+\frac{1}{\beta})}^{\text{Disappearance Term}}}_{\text{Coulomb Term}} \\ + \underbrace{\frac{2\beta R(Z+2i)}{R_{i+}\left[R^2+(Z+2i)^2/\gamma^2\right]}\delta(cT-R_{i+})}_{\text{Forward Radiatin Term}} \\ - \underbrace{\frac{2\beta R(Z-2i-1)}{R_{i-}[R^2+(Z-2i-1)^2/\gamma^2]}\delta(cT-\frac{1}{\beta}-R_{i-})}_{\text{Backward Radiation Term}} \end{array} \right\} \tag{20}$$

$$E_z = \sum_{i=-\infty}^{\infty} \left\{ \begin{array}{l} \gamma\left(\frac{Z+2i-\beta cT}{S_{i-}^{\ 3}} - \frac{Z+2i+\beta cT}{S_{i+}^{\ 3}}\right)u(cT-R_{i+})u(R_{0-}-cT+\frac{1}{\beta}) \\ - \frac{2\beta R^2}{R_{i+}\left[R^2+(Z+2i)^2/\gamma^2\right]}\delta(cT-R_{i+}) \\ + \frac{2\beta R^2}{R_{i-}[R^2+(Z-2i-1)^2/\gamma^2]}\delta(cT-\frac{1}{\beta}-R_{i-}) \end{array} \right\} \tag{21}$$

$$B_\phi = \sum_{i=-\infty}^{\infty} \left[\begin{array}{l} \beta\gamma\left(\frac{R}{S_{i-}^{\ 3}} + \frac{R}{S_{i+}^{\ 3}}\right)u(cT-R_{i+})u(R_{0-}-cT+\frac{1}{\beta}) \\ + \frac{2\beta R}{R^2+(Z+2i)^2/\gamma^2}\delta(cT-R_{i+}) \\ - \frac{2\beta R}{R^2+(Z-2i-1)^2/\gamma^2}\delta(cT-\frac{1}{\beta}-R_{i-}) \end{array} \right] \tag{22}$$

In Eq. (20), we brace out the terms in the early definition. The summations over all *i* terms take care of all reflected fields.

We now can see the electric field profile "movies" in Z-R coordinate generated by Mathcad. For all plots, the arrow at each grid only represents the electric field direction at that point. All arrows have same length, so each electric field vector is normalized at each grid. The left and right boundaries of the plot are the positions of the first and second conducting planes. The source charge moves at a velocity of β=0.84. In order to show the spherical wavefronts clearly the thickness of the wavefronts have been arbitrarily set into a 1% of the gap distance.

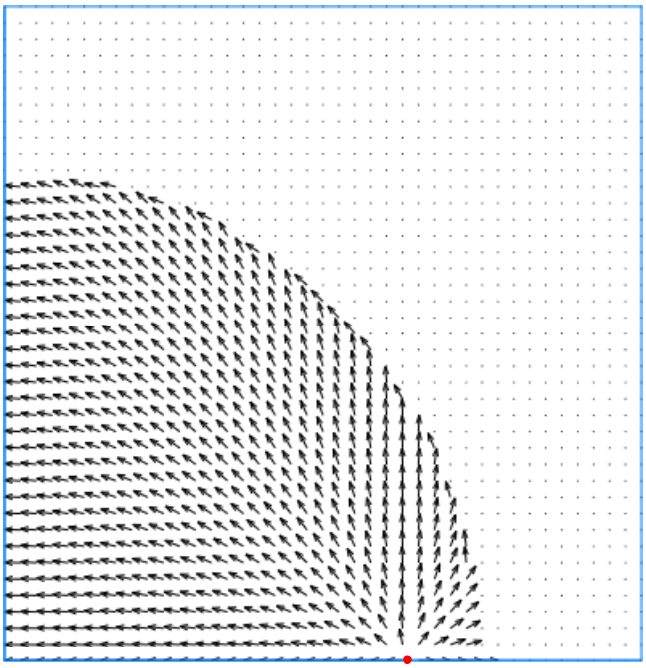

Electric vector plot at T=0.75/c

Figure 3: In this frame, at T=0.75/c, the red dot represents the positive source charge position.

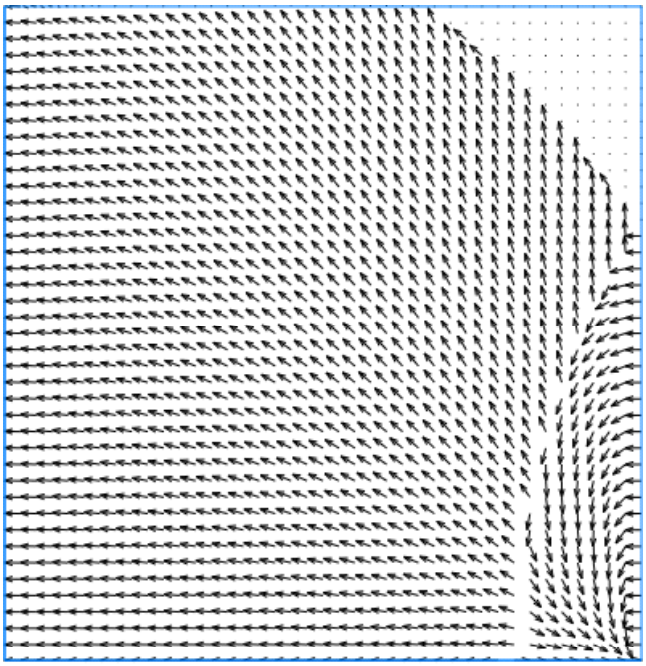

Electric vector plot at T=1.2/c

Figure 4: In this frame, at T=1.2/c, the positive charge is just striking the second conducting plate. The first reflected wave has shown up, a negative image charge represented its source just cancels the positive image charge created at this point for a backward radiation wave. So there is no net image charge coming back after this moment.

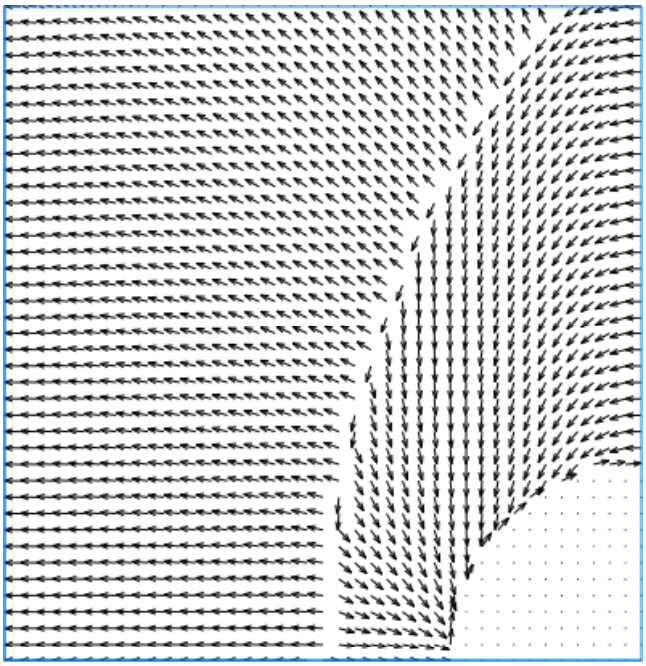

Electric vector plot at T=1.5/c

Figure 5: In this frame, at T=1.5/c, Coulomb filed lost its information within the backward radiation wavefront. All first-reflected field lines have to return to second conducting plate through the backward radiation field lines due to no image charge present here.

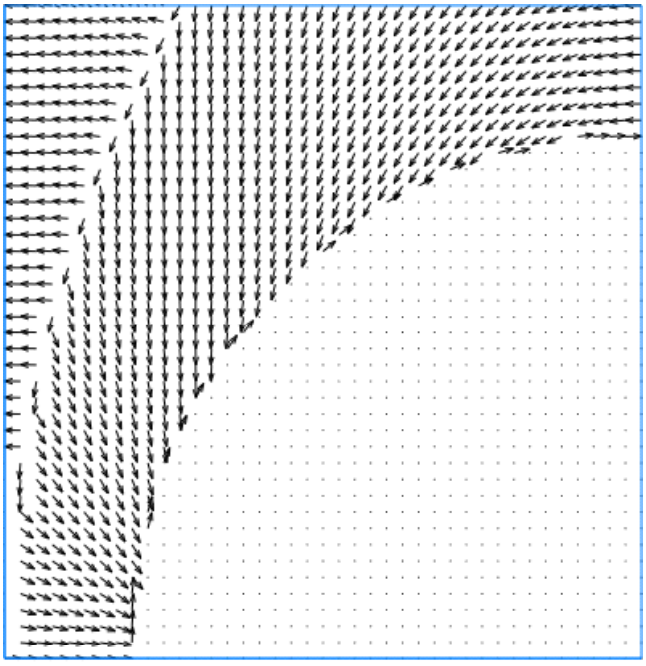

Electric vector plot at T=2.0/c

Figure 6: In this frame, at T=2/c. backward radiation propagates to the left, left a field vacuum behind.

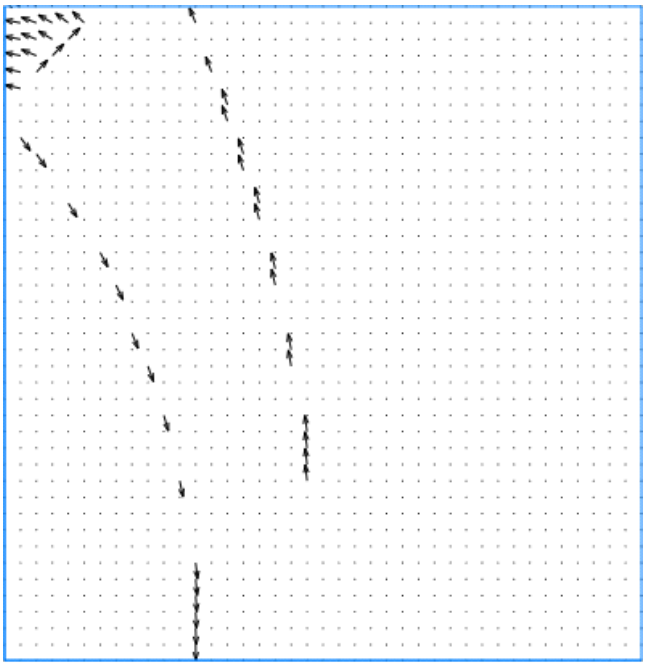

Electric vector plot at T=2.5/c

Figure 7: In this frame, at T=2.5/c, second-reflected forward radiation wave and first-reflected backward radiation wave have shown up. The Coulomb field has moved to up-left corner.

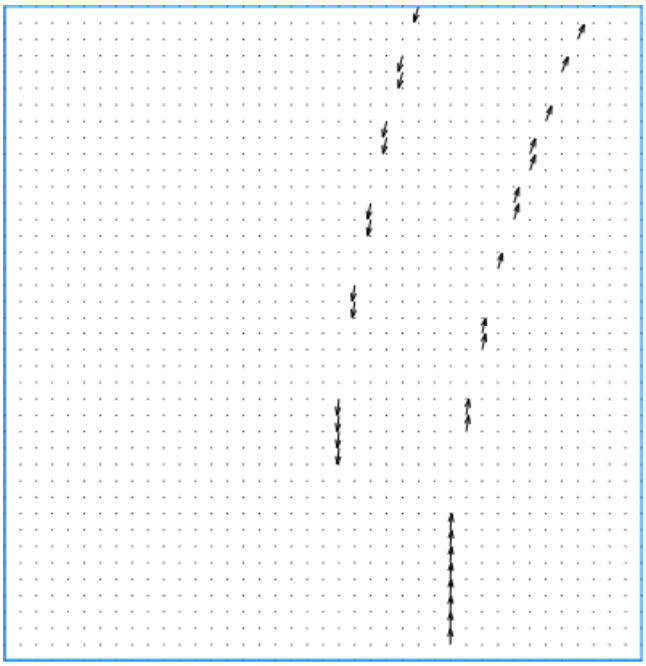

Electric vector plot at T=3.5/c

Figure 8: In this frame, at T=3.5/c, only reflected radiation waves left.

4. Green's Function of Wake-potential

So far, we have only worked on the point charge generated wakefields. A witness particle following the source particle to see its wakefields to gain or lose energy is the wake-potential. The integration of the wakefields calls Green's Function of Wake-potential.

The longitudinal wake-potential is:

$$w_{\delta //}(r,s)=\int_0^g e_z(r,z,t=\frac{z+s}{\beta c})dz \tag{23}$$

The transverse wake-potential can be expressed as:

$$w_{\delta\perp}(r,s)=\int_0^g\left[e_r(r,z,t=\frac{z+s}{\beta c})-\beta c b_\phi(r,z,t=\frac{z+s}{\beta c})\right]dz \tag{24}$$

As the conventional definition, $s>0$ is the distance of witness particle behind source particle, $s<0$ is the distance of witness particle ahead of source particle. $w_{\delta //}>0$ means a positive witness charge is accelerated, $w_{\delta //}<0$ means decelerated. $w_{\delta\perp}>0$ means a positive witness charge is defocused, $w_{\delta\perp}<0$ means focused.

Now we define normalized wake-potential and normalized distance:

$$W\equiv\frac{4\pi\varepsilon_0 g}{q}w \qquad S\equiv\frac{s}{g} \tag{25}$$

The normalized longitudinal wake-potential is:

$$W_{\delta //}(R,S)=\int_0^1 E_z(Z,R,T=\frac{Z+S}{\beta c})dZ \tag{26}$$

The normalized transverse wake-potential is:

$$W_{\delta\perp}(R,S)=\int_0^1\left[E_r(Z,R,T=\frac{Z+S}{\beta c})-\beta B_\phi(Z,R,T=\frac{Z+S}{\beta c})\right]dZ \tag{27}$$

When we integrate the field (26) and (27) analytically over the step functions and the Delta functions, there is a **causality** issue. That is when the witness particle starts seeing the source particle generated fields, and when the witness particle stops seeing the fields (Of course, you can do the integration numerically to avoid the problem). In Appendix A, we demonstrated in detail how to do the integration analytically, in which, gives more clearly physical picture of the causality issue. Since the algebra is very complicated, we only show the result plots here. Interesting readers can refer to Appendix A for causality algorithm and Appendix B for a Mathcad programming.

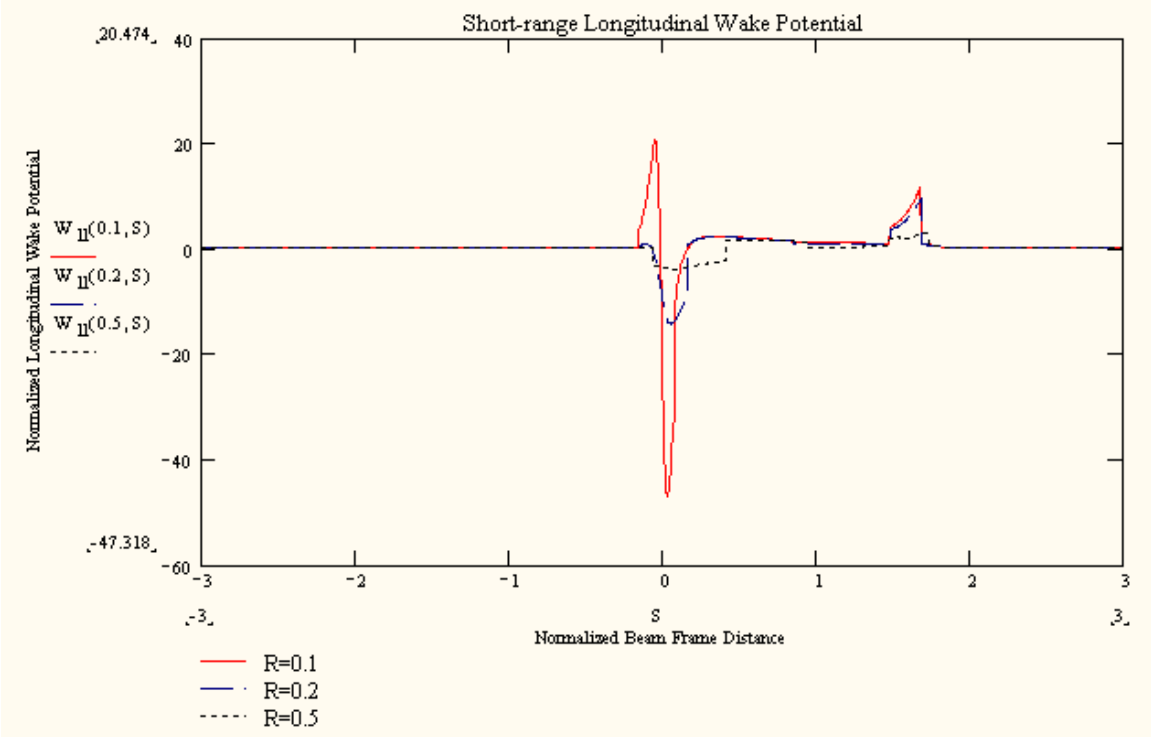

Figure 9: Short-range longitudinal wake-potential generated by a positive point charge moving (with $\beta=v/c=0.84$) between two conducting plates. Here R is the ratio of particle off-axis distance to the plate gap.

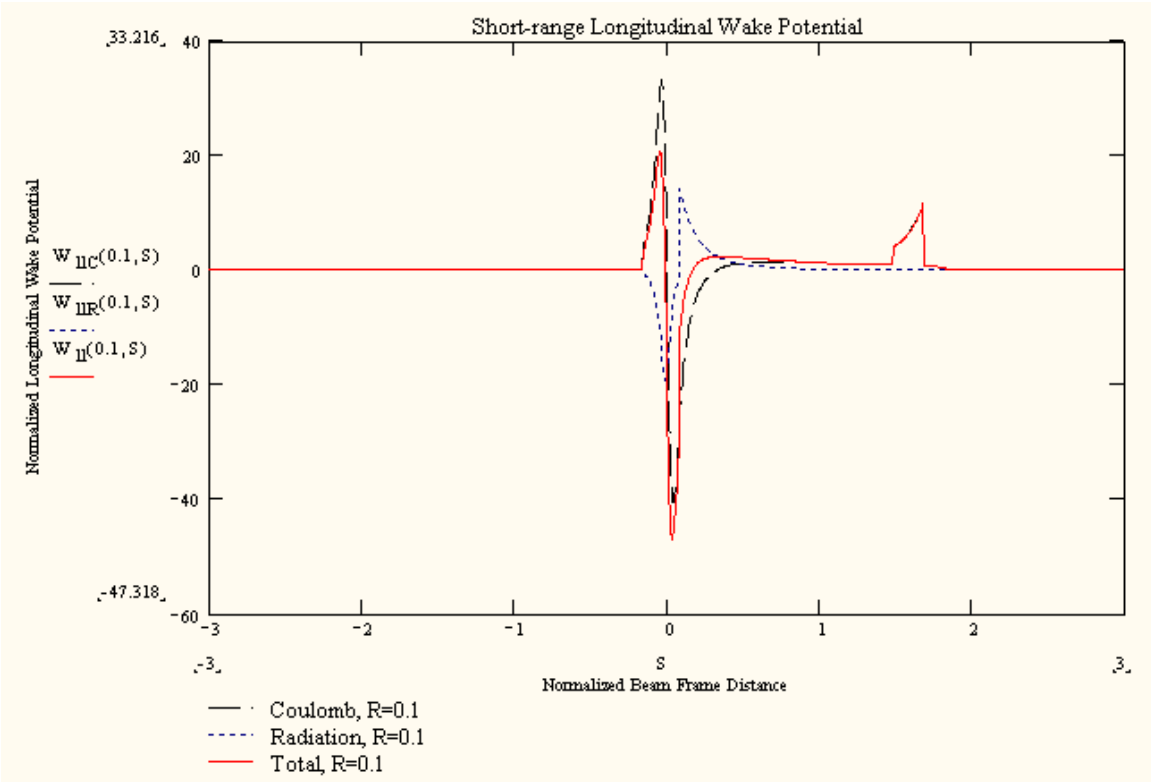

Figure 10: Coulomb and radiation wake-potentials shown separately for the case of R=0.1.

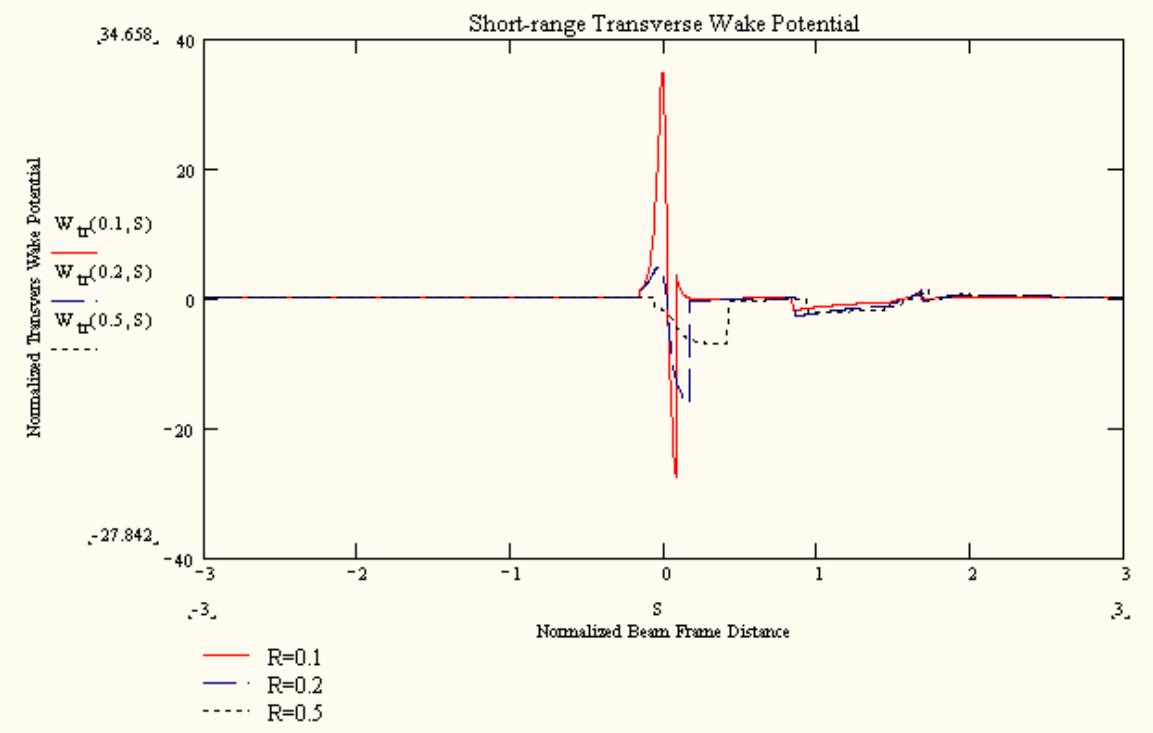

Figure 11: Short-range transverse wake-potential generated by a positive point charge moving (with $\beta=v/c=0.84$) between two conducting plates. Here R is the ratio of particle off-axis distance to the plate gap.

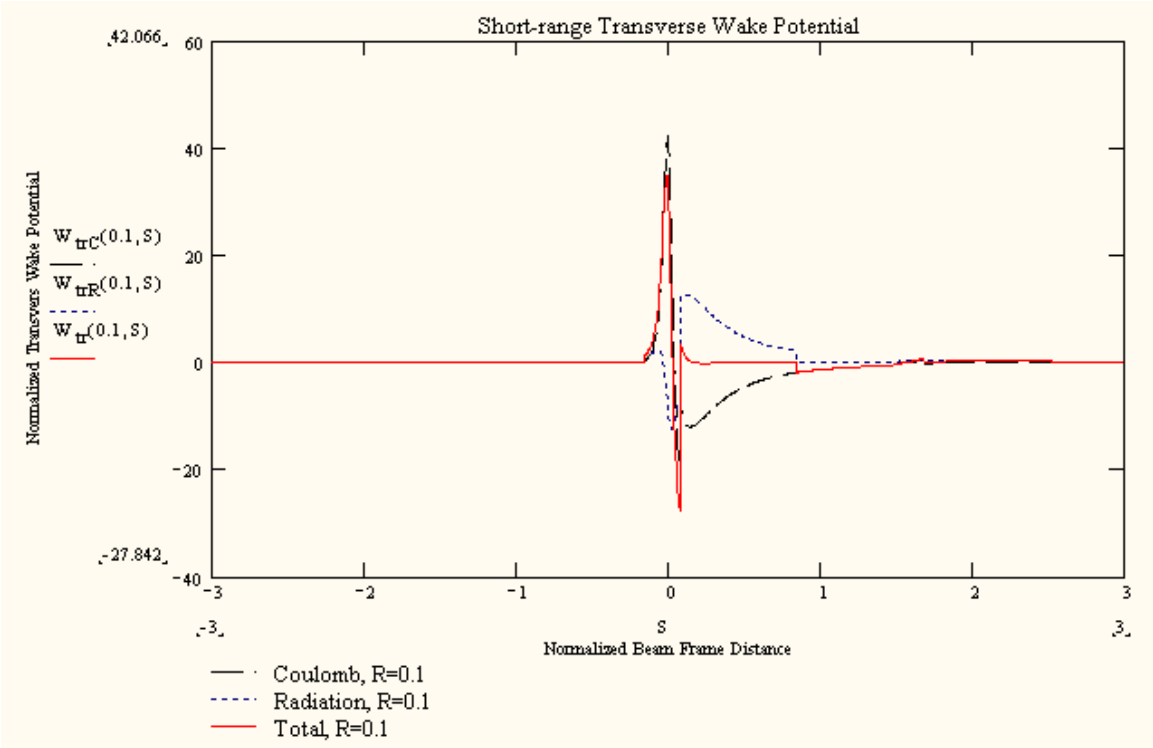

Figure 12: Coulomb and radiation wake-potentials shown separately for the case of R=0.1.

5. Wake-potential of a Gaussian Bunch Beam:

Once we know the Green's function of the wake-potential $w_\delta(s)$, we can integrate it to get the wake-potential for any given bunch distribution $\lambda(\mathbf{r},t)$. A convenient definition is a line charge distribution in longitudinal direction with a total chare q:

$$\rho(r,z,\phi,t) = q\lambda(\beta ct - z) = q\lambda(s) \tag{28}$$

For a Gaussian bunch with charge density distribution:

$$\lambda(s) = \frac{1}{\sigma\sqrt{2\pi}}\exp\left(-\frac{(s-s_0)^2}{2\sigma^2}\right) \tag{29}$$

Here, σ is the beam RMS bunch length.

The wake-potential is given by

$$w(s) = \int_{-\infty}^{+\infty}\lambda(s-s_1)w_\delta(s_1)ds_1 = \frac{1}{\sigma\sqrt{2\pi}}\int_{-\infty}^{+\infty}\exp\left(-\frac{(s-s_0-s_1)^2}{2\sigma^2}\right)w_\delta(s_1)ds_1 \tag{30}$$

Please pay attention here, the lower integration limit is -∞, not a zero. That is the character of sub-relativistic wakefield. The radiation field can be ahead of the moving particle. The wake-potential has to count that contribution.

Now we use normalized parameters defined above, but redefine the relative coordinate S' normalized to the bunch length σ and a relative bunch length Σ normalized to the gap distance g.

$$S' \equiv \frac{s}{\sigma} \qquad S'_0 \equiv \frac{s_0}{\sigma} \qquad S'_1 \equiv \frac{s_1}{\sigma} \qquad \Sigma \equiv \frac{\sigma}{g} \tag{31}$$

The normalized longitudinal wake-potential for a Gaussian beam bunch is:

$$W_{//}(R,S') = \frac{1}{\sqrt{2\pi}}\int_{-\infty}^{+\infty}\exp\left(-\frac{(S'-S'_0-S'_1)^2}{2}\right)W_{\delta//}(R,S'_1\cdot\Sigma)dS'_1 \tag{32}$$

The normalized transverse wake-potential for a Gaussian beam bunch is:

$$W_{\perp}(R,S') = \frac{1}{\sqrt{2\pi}}\int_{-\infty}^{+\infty}\exp\left(-\frac{(S'-S'_0-S'_1)^2}{2}\right)W_{\delta\perp}(R,S'_1\cdot\Sigma)dS'_1 \tag{33}$$

Then short-range wake-potential longitudinal (32) and transverse (33) for different off-axis distance R can be computed by a third Mathcad program (see Appendix B for detail). Following plots show the examples with S'_0=5, Σ=0.1918 case. It is a simulation of a bunched muon beam (with β=0.84, σ=1.5cm) in an 805 MHz pillbox cavity (with radius=14.28cm, g=7.821cm) in the muon cooling cannel for a muon collider.

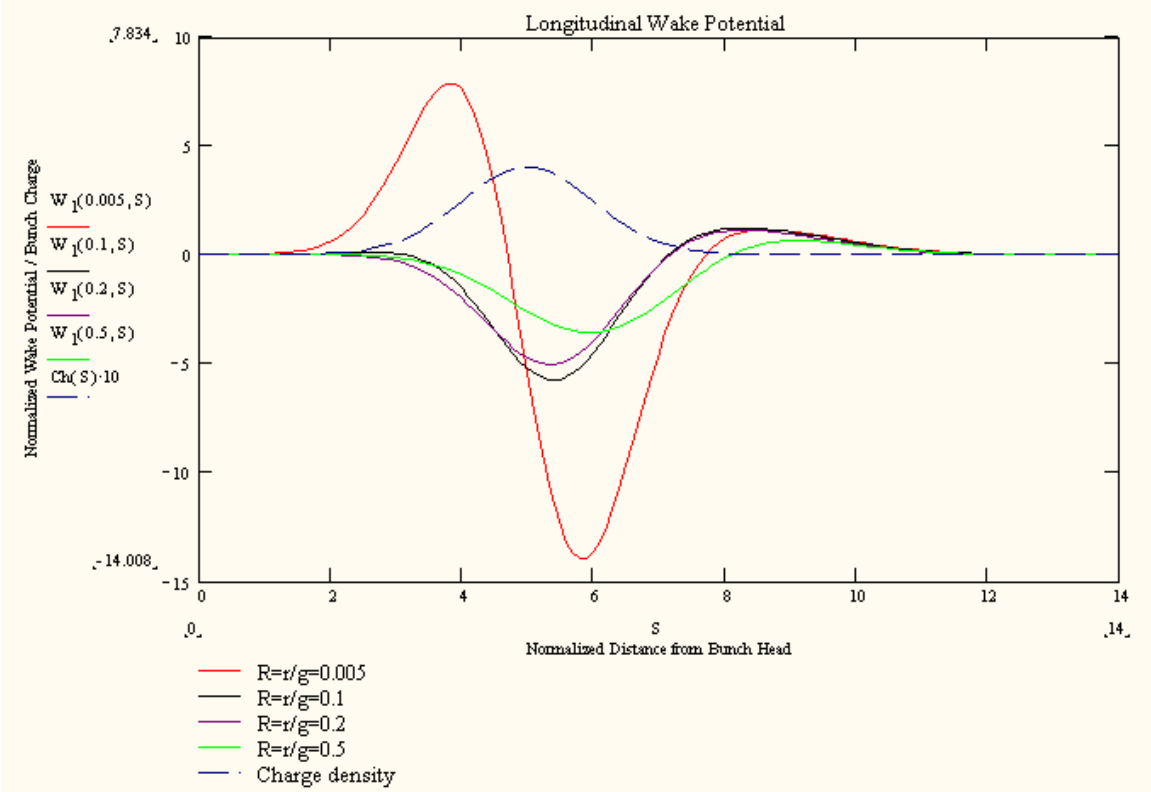

Figure 13: Normalized longitudinal wake-potential for a Gaussian beam bunch with β=0.84, s_0=5σ, and σ/g=0.1918 for witness particle at different off-axis distances $R=r/g$. The charge density is multiplied by 10 in order to see the bunch shape in the graph scale.

The results Figs. (13) and (14) can be readily compared with MAFIA 3D and 2D codes or other wakefield calculation code like ABCI (2D) [5]. The comparisons can also validate these codes in short-range wakefield calculation.

6. Conclusions

The image charge algorithm is a very powerful and fundamental tool to analytically calculate the short-range wakes reflected between two conducting plates when a sub-relativistic beam passing through them. It provides a key to understand physical picture of both space charge and wakefield problems when a short beam bunch is inside of a RF cavity though we do not consider the beam dynamic with RF field here. It shows a very good agreement with MAFIA and ABCI simulation codes in the short-range wakefield calculations for a broad range of particle velocity [5]. This is the first analytical approach to validate those wakefield calculation codes in such a short-range. We have also leaned that the frequency mode analysis technique already proofed the MAFIA wakefield calculation in long-range. This long-range so far experienced is beyond the distance when the witness particle passes the 8σ of Gaussian bunch if the bunch starts from -5σ, or when the radial reflected wave reaches the witness particle, whichever is shorter. That means MAFIA (2D or 3D) is a very trustful tool to simulate the wakefield or impedance problem in any range for a complex beam component structure.

The image charge algorithm may not suit for a pipe-like structure, in which the cylindrical radius is much smaller than the longitudinal gap distance. In this case, the witness particle may first see the reflected waves from the radial wall instead of planar wall. The current method only applies to the planar mirror but not to the cylindrical mirror. The image charge method for the cylindrical mirror is very cumbersome. Because a single image ring charge relative to a source ring charge on axis could not satisfy the boundary

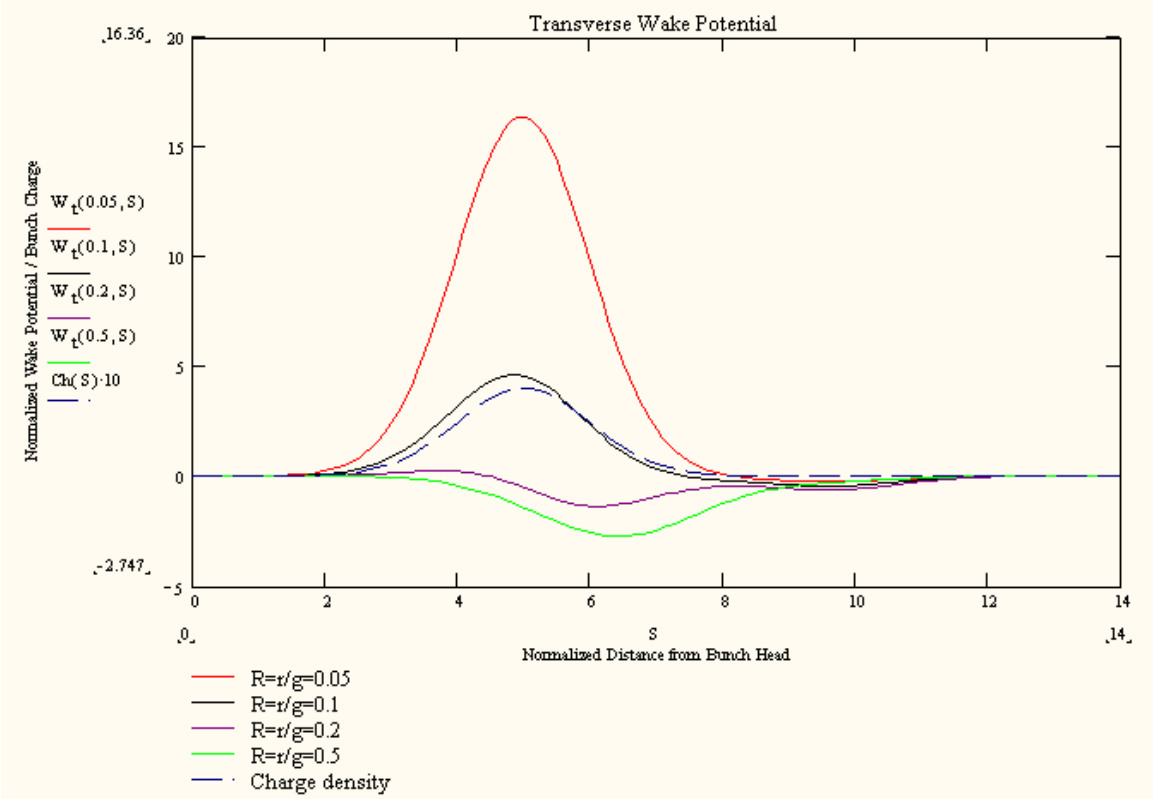

Figure 14: Normalized transverse wake-potential for a Gaussian beam bunch with β=0.84, s_0=5σ, and σ/g=0.1918 for witness particle at different off-axis distances $R=r/g$. The charge density is multiplied by 10 in order to see the bunch shape in the graph scale.

condition on the cylindrical surface. Even with a stack of image ring charges, the dynamic wavefronts from these image charges, when intercepting with the primary wavefront from the source charge on the mirror surface, may not exactly cancel each other. Even with reasonable numbers of reflected wavefronts, the mathematical expression for each wavefront is not as simple as in the point charge case. In this case, the diffraction method [10] could be used, but works done so far are only for the relativistic particle in long-range wakefield or impedance calculations. Anyhow, for a pipe like structure and for the sub-relativistic particle, we can rely on the MAFIA numerical simulation.

Acknowledgments

The author would like to thank Dr. R. Palmer for his constant encouragement and keen advice. He first pointed out the physics of the backward radiation and no electromagnetic information emitted after the charge left second conductor. The thanks should also go to Dr. J. Gallardo and Dr. S. Berg for their very helpful suggestions, and Dr. D. Li for his initial work on MAFIA simulation. All of them had many good discussions and comments during the course of this work.

References

[1] N. Holtkamp and D. Finley, ed., *A Feasibility Study of a Neutrino Source based on a Muon Storage Ring*, see http://www.fnal.gov/projects/muon_collider/nu-factory/fermi_study_after_april1st/, April 2000.
[2] J.N. Corlett, etc., *RF Accelerating Structures for the Muon Cooling Experiment*, Proc. of the 1999 Particle Accelerator Conference, New York, 1999, p3149.

[3] R. C. Fernow, *ICOOL: A Simulation Code for Ionization Cooling of Muon Beams*, Proc. of the 1999 Particle Accelerator Conference, New York, 1999, p3020.
[4] MAFIA User's Guide, CST GmbH, Darmstadt, Germany.
[5] H. Wang, *Sub-relativistic Wakefield in a Pillbox Cavity, Analytical Approach vs. MAFIA Simulation*, to be published with this tech note.
[6] A. Chao, *Physics of Collective Beam Instabilities in High Energy Accelerators*, Wiley Series in Beam Physics and Accelerator Technology (Wiley-Interscience, New York, 1993).
[7] A. Chao and P. L. Morton, *Physics Picture of the Electromagnetic Fields between Two Infinite Conducting Plates Produced by a Point Charge Moving at the Speed of Light*, SLAC Report PEP-105/SPEAR-182 (Feb. 1975).
[8] N. J. Carron, *Fields of Particles and Beams Exiting a Conductor*, A. J. Phys., submitted June 1998.
[9] N. J. Maresca, R. L. Liboff, *Field and Radiation due to a Charge Incident on a Conducting Plane*, J. Math. Phys. Vol. 16: 116-124 (Jan. 1975).
[10] A. Mostacci, L. Palumbo, F. Ruggiero, *Impedance and Loss Factor of a Coaxial Liner with Many Holes: Effect of the Attenuation*, Phys. Rev. ST-AB **2,** 124401 (1999).

Appendix A. Causality Issues in Wakefield Integration

When we analytically integrate (26) and (27), there are two Heaviside step functions $u(cT-R_{i+})$, $u(R_{0-}-cT+1/\beta)$, and two Delta functions $\delta(cT-R_{i+})$, $\delta(cT-1/\beta-R_{i-})$ need to be taken care of. For the Coulomb filed integration, we are dealing with the step functions, for example, you can only drop $u(cT-R_{i+})$ and $u(R_{0-}-cT+1/\beta)$ terms in the integration formula when the conditions $cT-R_{i+} > 0$ **AND** $R_{0-}-cT+1/\beta > 0$ satisfies. By making transformation $cT=(Z+S)/\beta$, we found the field is nonzero value only when Z and S are in certain range. That gives the integration limits extra conditional constrains. From the analysis shown later, we should find out that there are "open windows" for the witness particle to see the source particle Coulomb fields. Because the term $cT-R_{i+} > 0$ turns the field on, or the witness particle starts to see the retarded field of the source particle. Thus the term $R_{0-}-cT+1/\beta < 0$ i.e. $cT-R_{0-}-1/\beta > 0$ turns the field off, or the field inside of the conducting planes varnished after the source particle left the second conducting plane. This is the general causality issue and concept we discussed about.

Let's work on the appearance term, by solving the inequality:

$$cT - R_{i+} > 0 \tag{A1}$$

The discriminant is

$$\Delta = 4\beta^2\left[(S-2i)^2 + \frac{R^2}{\gamma^2}\right] \overbrace{\geq 0}^{always} \tag{A2}$$

We got the solutions:

$$Z > \gamma^2\left[(2\beta^2 i - S) + \beta\sqrt{(S-2i)^2 + \frac{R^2}{\gamma^2}}\right] \equiv Z_1(S,R,i) \quad \text{i.e.} \quad Z > Z_1(S,R,i) \tag{A3}$$

OR

$$Z < \gamma^2\left[(2\beta^2 i - S) - \beta\sqrt{(S-2i)^2 + \frac{R^2}{\gamma^2}}\right] \equiv Z_2(S,R,i) \quad \text{i.e. } Z < Z_2(S,R,i) \tag{A4}$$

Remember the transformation

$$cT = \frac{Z+S}{\beta} \overset{\text{always}}{\geq} 0 \tag{A5}$$

We can define the

$$Z_9(S) = -S \tag{A6}$$

The (A5) means $Z>Z_9(S)$. The functions of $Z_1(S,R,i)$, $Z_2(S,R,i)$ and $Z_9(S)$ can be drawn in a *Z-S* plot by Mathcad in Figure 15. We can conclude that $Z_2(S,R,i)$ does not have any physical meaning. That applies to any *R* and *i*.

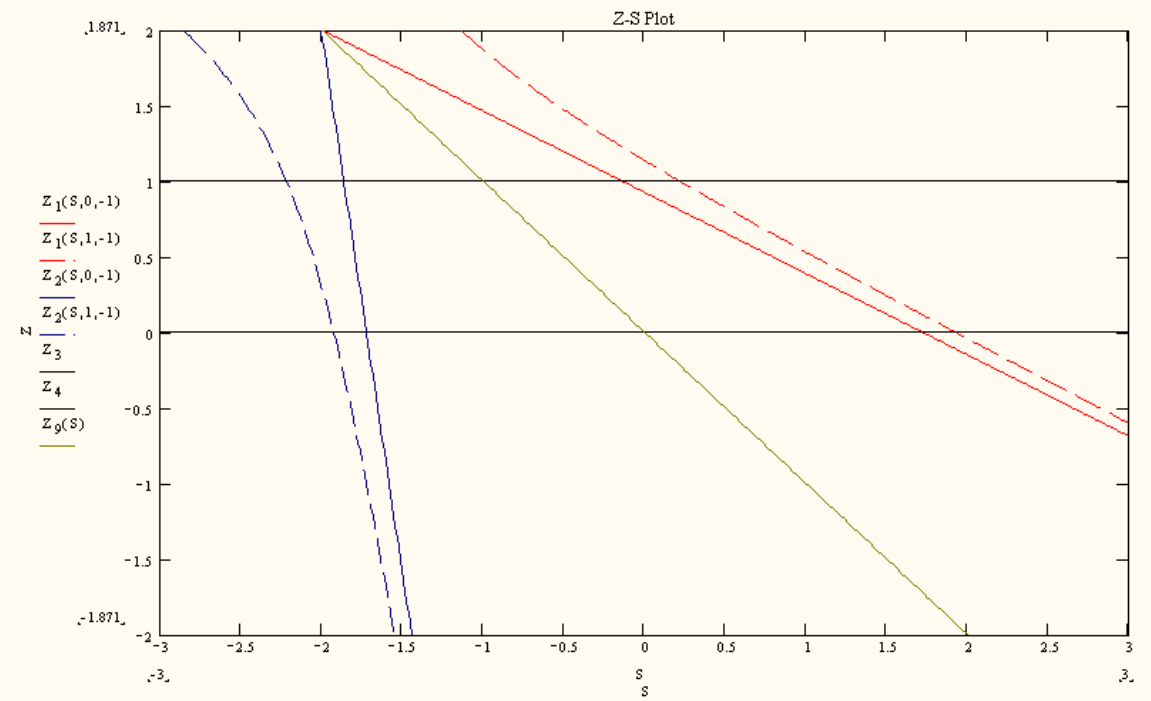

Figure 15: Work on the Z-S plot to determine the branch limit on appearance term (i=-1, β=0.86, R=0 or 1).

Let's work on the disappearance term, by solving the inequality:

$$R_{0-} - cT + \frac{1}{\beta} > 0 \tag{A7}$$

The discriminant is

$$\Delta = 4\beta^2\left(S^2 + \frac{R^2}{\gamma^2}\right)\overbrace{\geq 0}^{always} \tag{A8}$$

We got the solution:

$$Z_5(S,R) \equiv 1 - S\gamma^2 - \beta\gamma\sqrt{S^2\gamma^2 + R^2} < Z < 1 - S\gamma^2 + \beta\gamma\sqrt{S^2\gamma^2 + R^2} \equiv Z_6(S,R)$$

i.e. $Z_5(S,R) < Z < Z_6(S,R)$ (A9)

Remember that the backward radiation only happens after the source particle exiting the second plate. So

$$cT = \frac{Z+S}{\beta} > \frac{1}{\beta} \tag{A10}$$

We can define

$$Z_{10}(S) = 1 - S \tag{A11}$$

The functions of $Z_5(S,R)$, $Z_6(S,R)$ and $Z_{10}(S)$ can be drawn in a *Z-S* plot by Mathcad in Figure 16. We can conclude that $Z_5(S,R)$ does not have any physical meaning either. That applies to any *R*.

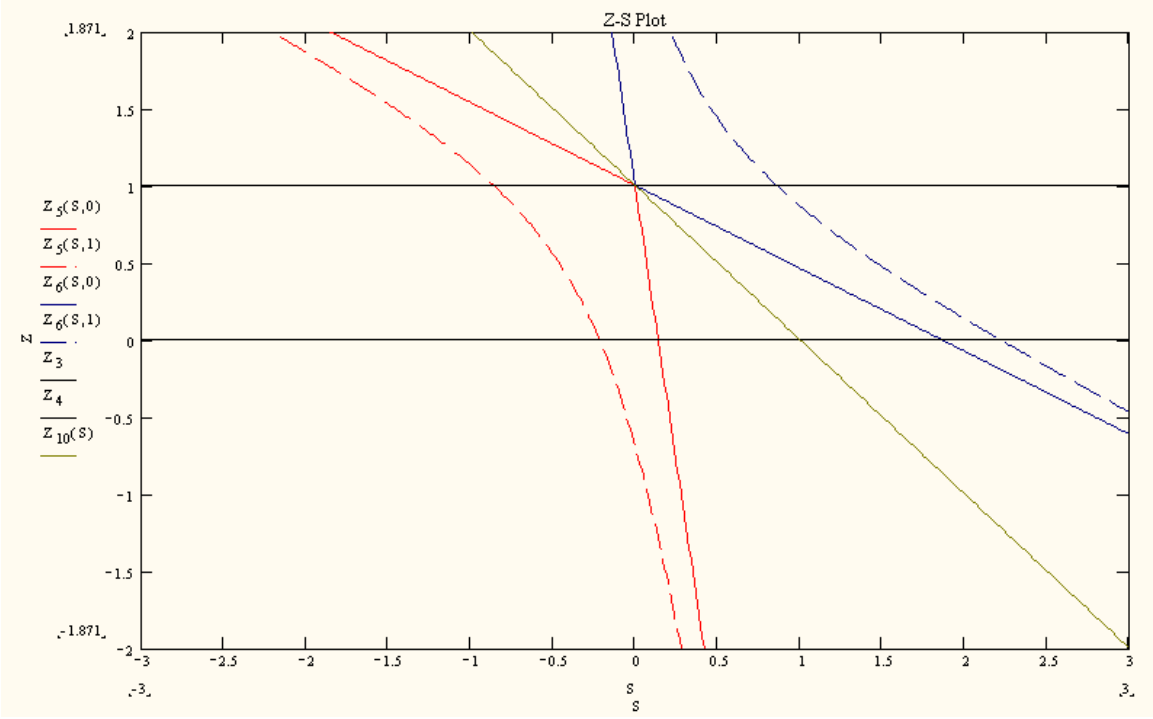

Figure 16: Work on the Z-S plot to determine the branch limit on disappearance term (β=0.86, R=0 or 1).

Remember that we are only interested in the fields between the two conducting plates, i.e. Z=0 to 1 range. We now define:

$$Z_3 = 0 \tag{A12}$$

And

$$Z_4 = 1 \tag{A13}$$

On the Z-S plot, let's work on the solution areas for the appearance term and disappearance term. We have found only functions $Z_1(S,R,i)$, $Z_6(S,R,i)$ have physical meanings. Because any radiation wavefront shown between the conducting planes is only half sphere. In order to see the Coulomb field within the forward radiation wavefront and beyond backward radiation wavefront, the witness particle is always in favor of $+S$ side. That means the witness particle behind the source particle is always easy to see the most portion of Coulomb field left behind source particle. So we only take (A3) and (A9, right) for the solution. However, for a small β or R, the $Z_1(S,R,i)$ still can be on $-S$ side. Because the radiation can catch the slow witness particle before it moves out of second plane.

For the appearance terms, the interception points between Z_3 and $Z_1(S,R,i)$ can be obtained analytically by solving $Z_1(S,R,i)=0$:

$$S_{31}(R,\beta,i) = \beta\sqrt{4i^2 + R^2} \tag{A14}$$

The interception between Z_4 and $Z_1(S,R,i)$:

$$S_{41}(R,\beta,i) = -1 + \beta\sqrt{(2i+1)^2 + R^2} \tag{A15}$$

For the disappearance terms, the interception between Z_3 and $Z_6(S,R)$ can be obtained analytically by solving $Z_6(S,R)=0$:

$$S_{36}(R,\beta) = 1 + \beta\sqrt{1 + R^2} \tag{A16}$$

The interception between Z_4 and $Z_6(S,R)$:

$$S_{46}(R,\beta) = \beta R \tag{A17}$$

The condition (A3) AND (A9, right) requires to find a common area in Z-S plot between the lines from Z_1 to Z_6 in S and from Z_3 to Z_4 in Z. The Figure 17 shows this common area for β=0.86 example, an "open window" for witness particle to see the Coulomb field in source term (i=0). At the $-S$ side of Z-S plot, there is a possibility to have a window area, like Figure 18, β=0.4 case.

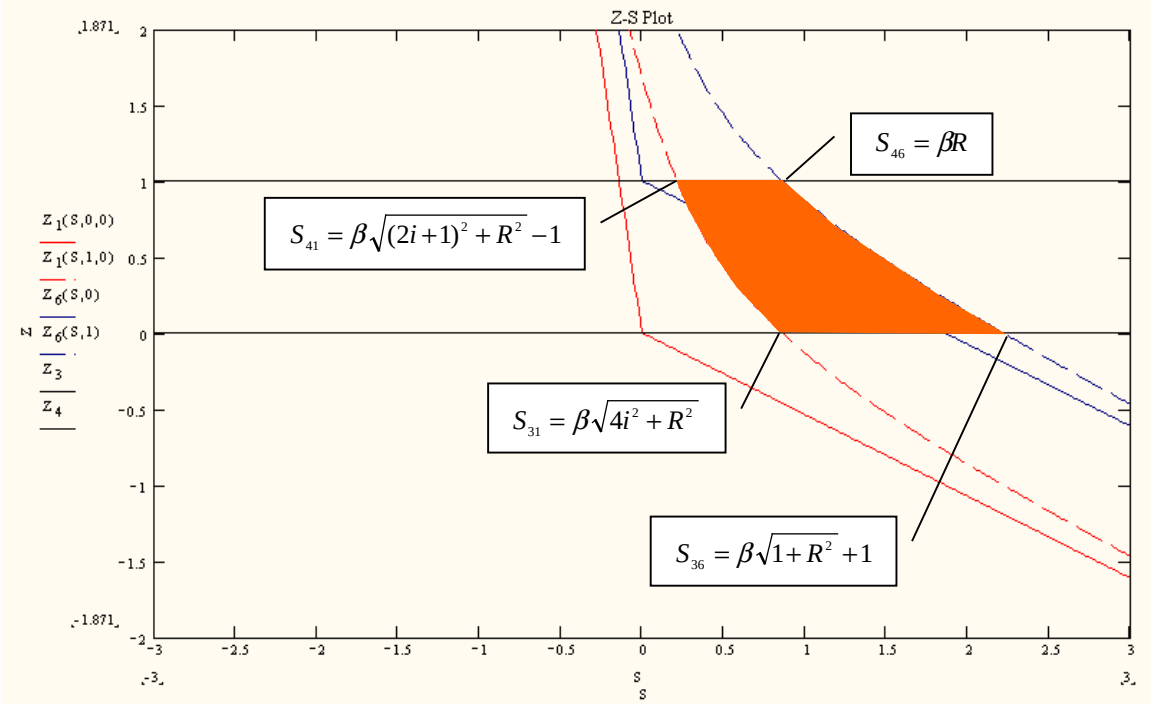

Figure 17: The "open window" in Z-S plot for β=0.86, i=0.

From Figures 17, 19 and 20, we can see that as the $|i|$ goes up, i.e. i=0, -1, +1, -2, +2…, the window area becomes smaller and smaller. After a certain $|i|$ value, the window disappears. The condition for the window disappearance is when:

$$S_{31} > S_{36} \quad \text{i.e.} \quad \beta\sqrt{4i^2 + R^2} > 1 + \beta\sqrt{1+R^2} \tag{A18}$$

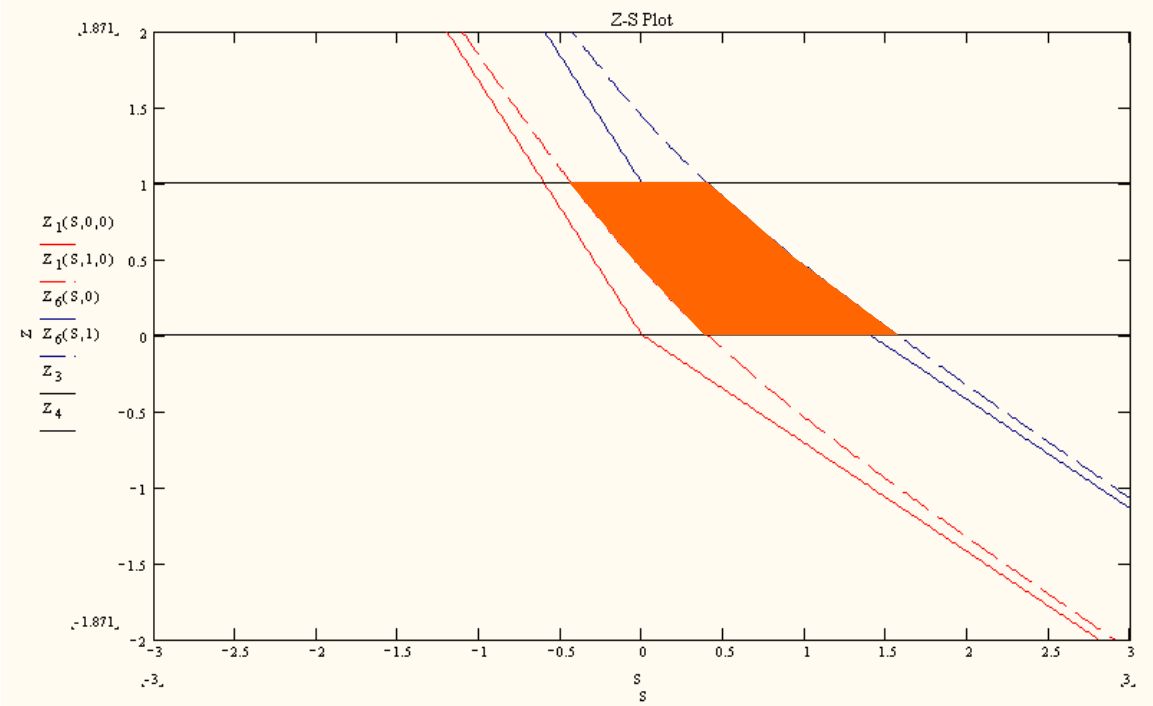

Figure 18: The "open window" in Z-S plot for β=0.4, i=0.

The solution of the (A18) is:

$$|i| > \frac{1}{2}\sqrt{1+\frac{1}{\beta^2}+\frac{2\sqrt{1+R^2}}{\beta}} \qquad \text{(A19)}$$

From (A19), we can see that as the β decreases, or as the source particle becomes more static, the $|i|$ requires to increase. That means the window numbers seen by the witness particle becomes larger, or the witness particle sees more reflected static fields. When the off-axis distance R increases, the window numbers becomes larger too.

Next, we are going to determine the window dimensions. That is to determine the integration low and high limits for (26) and (27).

The integration limits can be divided into different areas. When

$$S_{41} \le S_{46} \quad \text{i.e.} \quad -1+\beta\sqrt{(2i+1)^2+R^2} \le \beta R \qquad \text{(A20)}$$

AND

$$S_{46} \le S_{31} \le S_{36} \quad \text{i.e.} \quad \beta R \le \beta\sqrt{4i^2+R^2} \le 1+\beta\sqrt{1+R^2} \qquad \text{(A21)}$$

satisfied, the integration limits becomes three areas. The first area is from Z_1 to Z_4=1. The second area is from Z_1 to Z_6. The third area is from Z_3=0 to Z_6.
The solution for (A20) AND (A21) are

$$\left|2i+1\right| \le \frac{\sqrt{1+2\beta R}}{\beta} \qquad \text{(A22)}$$

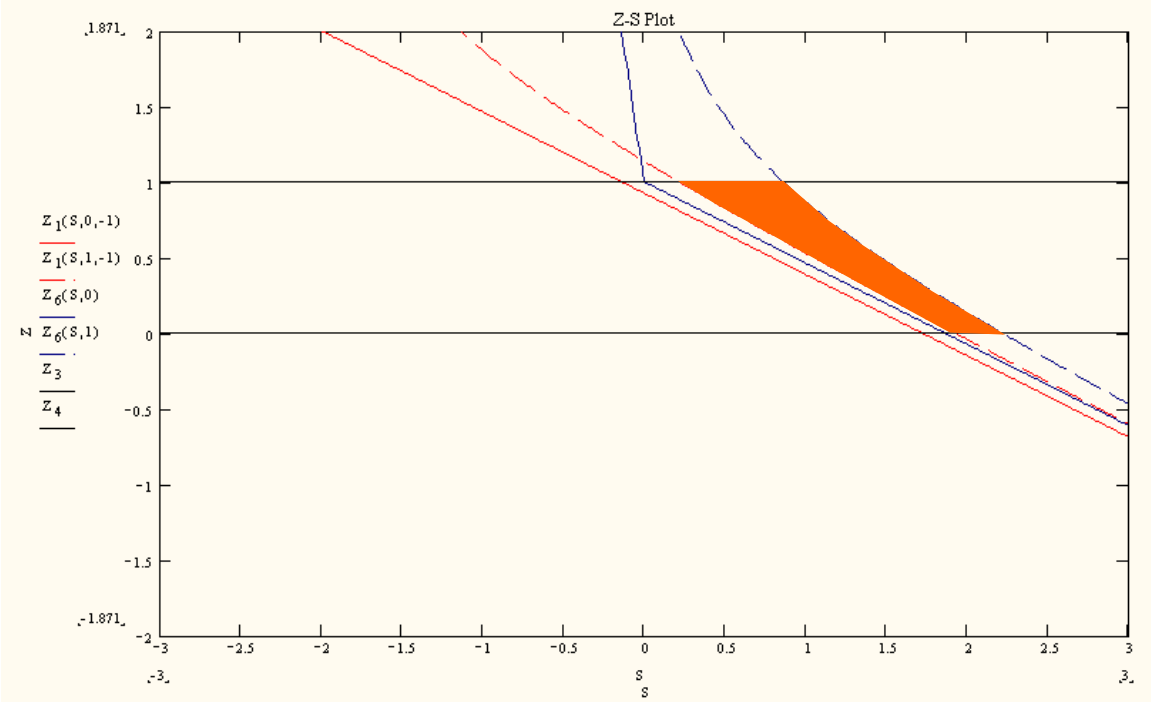

Figure 19: The "open window" in Z-S plot for β=0.86, i=-1.

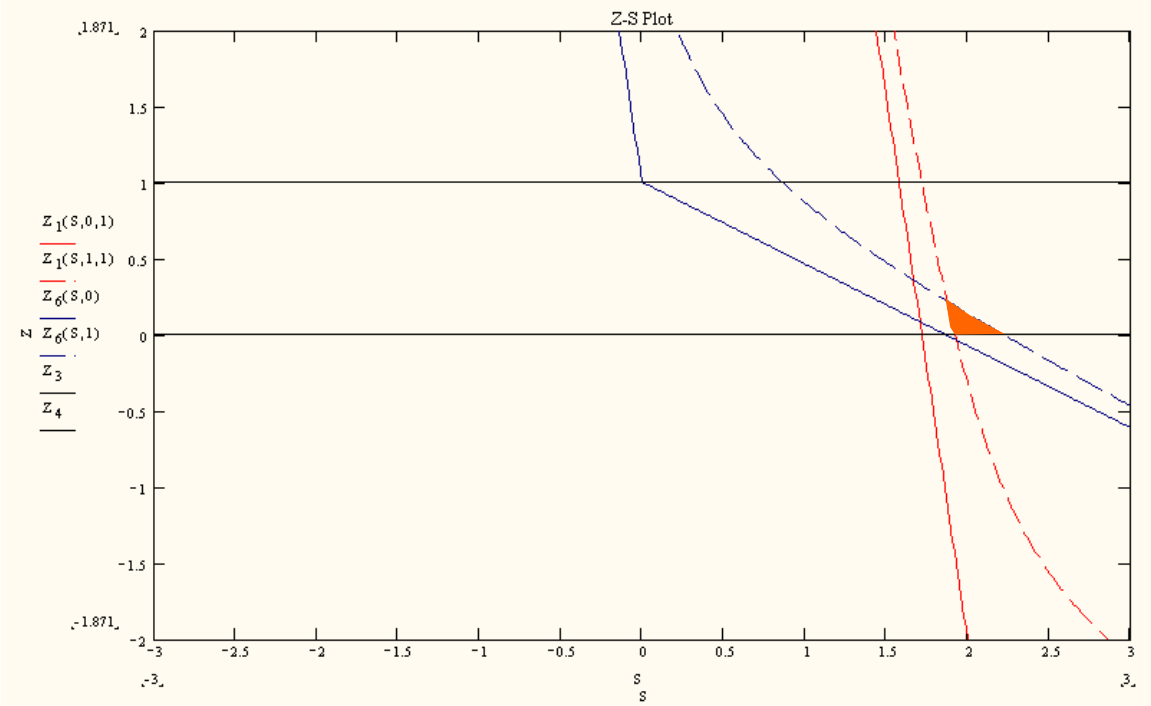

Figure 20: The "open window" in Z-S plot for β=0.86, i=1.

AND

$$|i| \le \frac{1}{2}\sqrt{1+\frac{1}{\beta^2}+\frac{2\sqrt{1+R^2}}{\beta}} \qquad \text{(A23)}$$

We can see that when $S_{31}=S_{46}$, $i=0$, which is the special case (two areas) of three areas solution.

When the (A20) changes the sign direction, that is

$$S_{41} > S_{46} \quad \text{i.e.} \quad -1+\beta\sqrt{(2i+1)^2+R^2} > \beta R \qquad \text{(A24)}$$

AND (A21) conditions satisfied, the integration limits reduced into two areas. The first area is from Z_1 to Z_6. The second area is from $Z_3=0$ to Z_6.

The integration limits or window dimensions for Coulomb fields can be summarized in Table 1.

S_{low}	S_{high}	Z_{low}	Z_{high}	Conditions
$\beta\sqrt{(2i+1)^2+R^2}-1$	βR	Z_1	1	$\lvert 2i+1\rvert \le \frac{\sqrt{1+2\beta R}}{\beta}$ AND
βR	$\beta\sqrt{4i^2+R^2}$	Z_1	Z_6	$\lvert i\rvert \le \frac{1}{2}\sqrt{1+\frac{1}{\beta^2}+\frac{2\sqrt{1+R^2}}{\beta}}$
$\beta\sqrt{4i^2+R^2}$	$\beta\sqrt{1+R^2}+1$	0	Z_6	
X[#]	$\beta\sqrt{4i^2+R^2}$	Z_1	Z_6	$\lvert 2i+1\rvert > \frac{\sqrt{1+2\beta R}}{\beta}$ AND
$\beta\sqrt{4i^2+R^2}$	$\beta\sqrt{1+R^2}+1$	0	Z_6	$\lvert i\rvert \le \frac{1}{2}\sqrt{1+\frac{1}{\beta^2}+\frac{2\sqrt{1+R^2}}{\beta}}$
No Windows Appear				$\lvert i\rvert > \frac{1}{2}\sqrt{1+\frac{1}{\beta^2}+\frac{2\sqrt{1+R^2}}{\beta}}$

Table 1: "Open window" dimensions of witness particle to see the source particle Coulomb field in the Z-S plot. Here $Z_1 = \gamma^2\left[(2\beta^2 i - S)+\beta\sqrt{(S-2i)^2+\frac{R^2}{\gamma^2}}\right]$ and $Z_6 = 1 - S\gamma^2 + \beta\gamma\sqrt{S^2\gamma^2+R^2}$.

Now we can integrate the Coulomb field term by term.

The Coulomb wake-potential is

$$W_{//C}(R,S) = \sum_{i=-j}^{j} F_{//C}(Z_{high}) - F_{//C}(Z_{low}) \qquad \text{See condition in the shaded area in Table 1} \qquad \text{(A25)}$$

[#] X is the root of the equation $Z_1 = Z_6$.

Here $j = \text{integer}\left(\frac{1}{2}\sqrt{1+\frac{1}{\beta^2}+\frac{2\sqrt{1+R^2}}{\beta}}\right)$ (A26)

That means you do not need to calculate so many terms for a fast particle.

And $F_{//C}(Z)$ is the integration function of Coulomb field E_{ZC}, and it was found out

$$F_{//C}(Z) = \gamma\left\{\frac{2i-S}{\left[R^2+\gamma^2(S-2i)^2\right]^{3/2}}Z + \frac{1}{2\gamma^2\sqrt{R^2+\gamma^2(2Z+S+2i)^2}}\right\} \quad \text{(A27)}$$

The radiation fields (forward and backward) are just one-time contribution to the wake-potential at their wavefronts. The integration over the radiation fields is similar to but simpler than the Coulomb fields. We can solve the forward radiation wavefront position Z_1 by putting equal sign into (A1) and getting

$$Z_1(S,R,i) = \gamma^2\left[(2\beta^2 i - S) + \beta\sqrt{(S-2i)^2+\frac{R^2}{\gamma^2}}\right] \quad \text{(A28)}$$

OR

$$Z_2(S,R,i) = \gamma^2\left[(2\beta^2 i - S) - \beta\sqrt{(S-2i)^2+\frac{R^2}{\gamma^2}}\right] \quad \text{(A29)}$$

We know that only $Z_1(S,R,i)$ has a physical meaning.

In a similar way, we can solve the backward radiation wavefront position Z_7 by

$$cT - \frac{1}{\beta} - R_{i-} = 0 \quad \text{(A30)}$$

We get

$$Z_7(S,R,i) = -\gamma^2\left[S - \frac{1}{\gamma^2} + 2\beta^2 i - \beta\sqrt{(S+2i)^2+\frac{R^2}{\gamma^2}}\right] \quad \text{(A31)}$$

OR

$$Z_8(S,R,i) = -\gamma^2\left[S - \frac{1}{\gamma^2} + 2\beta^2 i + \beta\sqrt{(S+2i)^2+\frac{R^2}{\gamma^2}}\right] \quad \text{(A32)}$$

In a similar way to work on the $Z_5(S,R)$, from Figure 21, we can rule the $Z_8(S,R,i)$ out , which does not have any physical meaning.

It is obviously that $Z_8(S,R,0)=Z_5(S,R)$ and $Z_7(S,R,0)=Z_6(S,R)$. So $Z_7(S,R,i)$ is the backward radiation wavefront positions in general for any R and i.

The interception between $Z_7(S,R,i)$ and $Z_3=0$ can be found

$$S_{37} = 1+\beta\sqrt{4i(i+1)+1+R^2} \tag{A33}$$

The interception between $Z_7(S,R,i)$ and $Z_4=1$ can be found

$$S_{47} = \beta\sqrt{R^2+4i^2} \tag{A34}$$

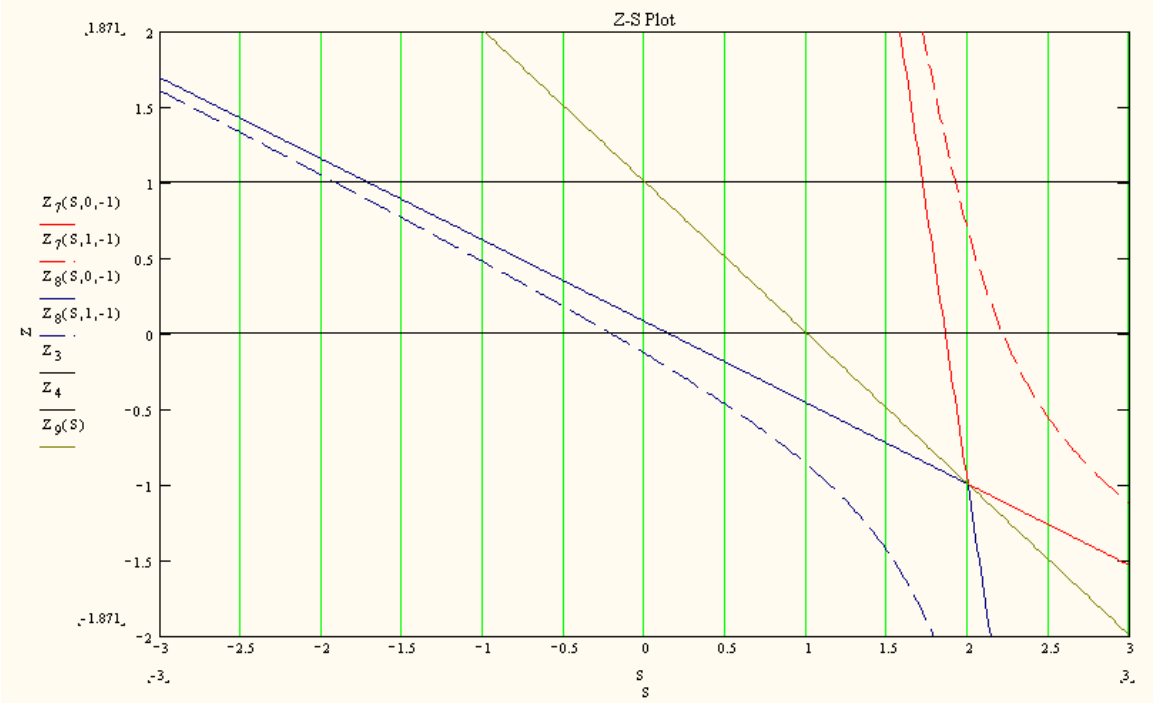

Figure 21: Work on the Z-S plot to determine radiation wavefront position. In this example, β=0.86, i=-1.

We can see that $S_{47}(R,\beta,i) \overset{always}{\geq} 0$. That means the witness particle ahead of the source particle could not see any backward radiation. That is because when the backward radiation generated, the witness particle already left the second plate. The radiation wavefront positions can be summarized in Table 2.

The radiation wake-potential is:

$$W_{//R}(R,S) = \begin{cases} \Phi_{//F}(Z_1) & if \quad \beta\sqrt{(2i+1)^2+R^2}-1 \le S \le \beta\sqrt{4i^2+R^2} \\ + \quad \Phi_{//B}(Z_7) & if \quad \beta\sqrt{4i^2+R^2} \le S \le \beta\sqrt{(2i+1)^2+R^2} \\ 0 & Others \end{cases} \tag{A35}$$

Here $\Phi_{//F}(Z)$ is the integration function of forward radiation field E_{ZF}.

$$\Phi_{//F}(Z) = -\sum_{i=-\infty}^{\infty} \frac{2\beta R^2}{\sqrt{R^2+(Z+2i)^2}\left[R^2+(Z+2i)^2/\gamma^2\right]} \frac{1}{\left|\frac{1}{\beta}-\frac{Z+2i}{\sqrt{R^2+(Z+2i)^2}}\right|} \tag{A36}$$

And $\Phi_{//B}(Z)$ is the integration function of backward radiation field E_{ZB}.

$$\Phi_{//B}(Z) = \sum_{i=-\infty}^{\infty} \frac{2\beta R^2}{\sqrt{R^2+(Z-2i-1)^2}\left[R^2+(Z-2i-1)^2/\gamma^2\right]} \frac{1}{\left|\frac{1}{\beta}-\frac{Z-2i-1}{\sqrt{R^2+(Z-2i-1)^2}}\right|} \tag{A37}$$

You do not need so many terms to calculate short-range radiation potentials either. A simple way to estimate it is to look at how many forward radiation and its reflection wavefronts have shown up between the parallel plates within the defined S range. Since the forward radiation always happens first, though its reflections may come later than the backward radiation, the forward radiation always starts with i=0 wave first. We require that

$$S \geq S_{low} \qquad \text{i.e.} \qquad S \geq \beta\sqrt{(2i+1)^2+R^2}-1 \tag{A38}$$

We got

$$|i| \leq \frac{1}{2}\sqrt{\left(\frac{S+1}{\beta}\right)^2 - R^2} - \frac{1}{2} \tag{A39}$$

S_{low}	S_{high}	$Z_{wavefront}$	Note
$\beta\sqrt{(2i+1)^2+R^2}-1$	$\beta\sqrt{4i^2+R^2}$	Z_1	Forward radiation
$\beta\sqrt{4i^2+R^2}$	$\beta\sqrt{(2i+1)^2+R^2}$	Z_7	Backward radiation
Others		No radiation can be seen	

Table 2: Radiation wavefront positions. Here $Z_1 = \gamma^2\left[(2\beta^2 i - S) + \beta\sqrt{(S-2i)^2+\frac{R^2}{\gamma^2}}\right]$,

$Z_7 = -\gamma^2\left[S - \frac{1}{\gamma^2} + 2\beta^2 i - \beta\sqrt{(S+2i)^2+\frac{R^2}{\gamma^2}}\right]$.

The total longitudinal wake-potential is the sum of the Coulomb and radiation potentials.

$$W_{//}(R,S) = W_{//C}(R,S) + W_{//R}(R,S) \tag{A40}$$

In a similar way, we can get total transverse wake-potential

$$W_{\perp}(R,S) = W_{\perp C}(R,S) + W_{\perp R}(R,S) \tag{A41}$$

$$W_{\perp C}(R,S)=\sum_{i=-j}^{j}F_{\perp C}(Z_{high})-F_{\perp C}(Z_{low})$$ See the condition in the shaded area in Table 1 (A42)

Here $j=\text{integer}\left(\frac{1}{2}\sqrt{1+\frac{1}{\beta^2}+\frac{2\sqrt{1+R^2}}{\beta}}\right)$ (A26)

And $F_{\perp C}(Z)$ is the integration function of Coulomb field E_{rC}-$\beta B_{\phi C}$, and it was found out

$$F_{\perp C}(Z)=\left\{\frac{R}{\gamma\left[R^2+\gamma^2(S-2i)^2\right]^{3/2}}Z-\frac{(1+\beta^2)\gamma(2Z+S+2i)}{2R\sqrt{R^2+\gamma^2(2Z+S+2i)^2}}\right\} \quad (A43)$$

$$W_{\perp R}(R,S)=\left\{\begin{array}{ll}\Phi_{\perp F}(Z_1) & if\quad \beta\sqrt{(2i+1)^2+R^2}-1\le S\le\beta\sqrt{4i^2+R^2}\\ +\quad \Phi_{\perp B}(Z_7) & if\quad \beta\sqrt{4i^2+R^2}\le S\le\beta\sqrt{(2i+1)^2+R^2}\\ 0 & Others\end{array}\right\} \quad (A44)$$

Here $\Phi_{\perp F}(Z)$ is the integration function of forward radiation field E_{rF}-$\beta B_{\phi F}$.

$$\Phi_{\perp F}(Z)=\sum_{i=-\infty}^{\infty}\frac{2\beta R}{\left[R^2+(Z+2i)^2/\gamma^2\right]}\left(\frac{Z+2i}{\sqrt{R^2+(Z+2i)^2}}-\beta\right)\frac{1}{\left|\frac{1}{\beta}-\frac{Z+2i}{\sqrt{R^2+(Z+2i)^2}}\right|} \quad (A45)$$

And $\Phi_{\perp B}(Z)$ is the integration function of backward radiation field E_{rB}-$\beta B_{\phi B}$.

$$\Phi_{\perp B}(Z)=-\sum_{i=-\infty}^{\infty}\frac{2\beta R}{\left[R^2+(Z-2i-1)^2/\gamma^2\right]}\left(\frac{Z-2i-1}{\sqrt{R^2+(Z-2i-1)^2}}-\beta\right)\frac{1}{\left|\frac{1}{\beta}-\frac{Z-2i-1}{\sqrt{R^2+(Z-2i-1)^2}}\right|} \quad (A46)$$

Appendix B. A Mathcad Program for Wake-potential Calculation

Short-range Wake-potential Produced by a Sub-relativistic Gaussian Bunch Passing through Two Parallel Conducting Plates (Green Function Integrated by Analytical Formulas).

H. Wang, 04/10/2000

1. Longitudinal Coulomb:

$\beta := 0.84$

$$\gamma := \frac{1}{\sqrt{1-\beta^2}}$$

$$Z_1(R,S,i) := \gamma^2 \cdot \left[\left(2\cdot\beta^2\cdot i - S\right) + \beta \cdot \sqrt{(S-2\cdot i)^2 + \frac{R^2}{\gamma^2}} \right]$$

$$Z_6(R,S) := 1 - S\cdot\gamma^2 + \beta\cdot\gamma\cdot\sqrt{S^2\cdot\gamma^2 + R^2}$$

$$F_{llCi}(Z,R,S,i) := \gamma \cdot \left[\frac{1}{2\cdot\gamma^2\cdot\sqrt{R^2+\gamma^2\cdot(2\cdot Z+S+2\cdot i)^2}} + \frac{2\cdot i - S}{\left[R^2+\gamma^2\cdot(S-2\cdot i)^2\right]^{1.5}}\cdot Z \right]$$

$$W_{llC1}(R,S,i) := \begin{cases} F_{llCi}(1,R,S,i) - F_{llCi}\left(Z_1(R,S,i),R,S,i\right) & \text{if } \beta\cdot\sqrt{(2\cdot i+1)^2+R^2} - 1 \le S \le \beta\cdot R \\ F_{llCi}\left(Z_6(R,S),R,S,i\right) - F_{llCi}\left(Z_1(R,S,i),R,S,i\right) & \text{if } \beta\cdot R < S < \beta\cdot\sqrt{4\cdot i^2+R^2} \\ F_{llCi}\left(Z_6(R,S),R,S,i\right) - F_{llCi}(0,R,S,i) & \text{if } \beta\cdot\sqrt{4\cdot i^2+R^2} \le S \le \beta\cdot\sqrt{1+R^2}+1 \\ 0 & \text{otherwise} \end{cases}$$

$$X(R,i) := \begin{cases} x \leftarrow 2 \\ \text{root}\left(Z_1(R,x,i) - Z_6(R,x), x\right) \end{cases}$$

$$W_{llC2}(R,S,i) := \begin{cases} F_{llCi}\left(Z_6(S,R),R,S,i\right) - F_{llCi}\left(Z_1(R,S,i),R,S,i\right) & \text{if } X(R,i) \le S \le \beta\cdot\sqrt{4\cdot i^2+R^2} \\ F_{llCi}\left(Z_6(R,S),R,S,i\right) - F_{llCi}(0,R,S,i) & \text{if } \beta\cdot\sqrt{4\cdot i^2+R^2} < S \le \beta\cdot\sqrt{1+R^2}+1 \\ 0 & \text{otherwise} \end{cases}$$

$$W_{llC}(R,S) := \begin{cases} j \leftarrow \text{round}\left(\frac{1}{2}\cdot\sqrt{1+\frac{1}{\beta^2}+2\cdot\frac{\sqrt{1+R^2}}{\beta}}\right) \\ W \leftarrow 0 \\ \text{for } i \in -j..j \\ \quad W \leftarrow W + \begin{cases} W_{llC1}(R,S,i) & \text{if } |2\cdot i+1| \le \frac{\sqrt{1+2\cdot\beta\cdot R}}{\beta} \\ W_{llC2}(R,S,i) & \text{otherwise} \end{cases} \\ W \end{cases}$$

2. Longitudinal Radiation:

$$Z_7(R,S,i) := -\gamma^2\cdot\left[2\cdot\beta^2\cdot i + S - \frac{1}{\gamma^2} - \beta\cdot\sqrt{(S+2\cdot i)^2+\frac{R^2}{\gamma^2}}\right]$$

$$\Phi_{llFi}(Z,R,S,i) := \frac{-2\cdot\beta\cdot R^2}{\sqrt{R^2+(Z+2\cdot i)^2}\cdot\left[R^2+\frac{(Z+2\cdot i)^2}{\gamma^2}\right]}\cdot\frac{1}{\left|\frac{1}{\beta}-\frac{Z+2\cdot i}{\sqrt{R^2+(Z+2\cdot i)^2}}\right|}$$

$$\Phi_{llBi}(Z,R,S,i) := \frac{2\cdot\beta\cdot R^2}{\sqrt{R^2+(Z-2\cdot i-1)^2}\cdot\left[R^2+\frac{(Z-2\cdot i-1)^2}{\gamma^2}\right]}\cdot\frac{1}{\left|\frac{1}{\beta}-\frac{Z-2\cdot i-1}{\sqrt{R^2+(Z-2\cdot i-1)^2}}\right|}$$

$$W_{llFi}(R,S,i) := \begin{cases} \Phi_{llFi}\left(Z_1(R,S,i),R,S,i\right) & \text{if } \beta\cdot\sqrt{(2\cdot i+1)^2+R^2}-1\le S\le\beta\cdot\sqrt{4\cdot i^2+R^2} \\ 0 & \text{otherwise} \end{cases}$$

$$W_{llBi}(R,S,i) := \begin{cases} \Phi_{llBi}\left(Z_7(R,S,i),R,S,i\right) & \text{if } \beta\cdot\sqrt{4\cdot i^2+R^2}\le S\le\beta\cdot\sqrt{(2\cdot i+1)^2+R^2} \\ 0 & \text{otherwise} \end{cases}$$

$$W_{llR}(R,S) := \left[\sum_{i=-7}^{7} W_{llFi}(R,S,i)+W_{llBi}(R,S,i)\right]$$

3. Longitudinal Total:

$$W_{ll}(R,S) := W_{llC}(R,S)+W_{llR}(R,S)$$

4. Transverse Coulomb:

$$F_{trCi}(Z,R,S,i) := \frac{R\cdot Z}{\gamma\cdot\left[R^2+\gamma^2\cdot(S-2\cdot i)^2\right]^{1.5}} - \frac{\left(1+\beta^2\right)\cdot\gamma\cdot(2\cdot Z+S+2\cdot i)}{2\cdot R\cdot\sqrt{R^2+\gamma^2\cdot(2\cdot Z+S+2\cdot i)^2}}$$

$$W_{trC1}(R,S,i) := \begin{cases} F_{trCi}(1,R,S,i)-F_{trCi}\left(Z_1(R,S,i),R,S,i\right) & \text{if } \beta\cdot\sqrt{(2\cdot i+1)^2+R^2}-1\le S\le\beta\cdot R \\ F_{trCi}\left(Z_6(R,S),R,S,i\right)-F_{trCi}\left(Z_1(R,S,i),R,S,i\right) & \text{if } \beta\cdot R<S<\beta\cdot\sqrt{4\cdot i^2+R^2} \\ F_{trCi}\left(Z_6(R,S),R,S,i\right)-F_{trCi}(0,R,S,i) & \text{if } \beta\cdot\sqrt{4\cdot i^2+R^2}\le S\le\beta\cdot\sqrt{1+R^2}+1 \\ 0 & \text{otherwise} \end{cases}$$

$$W_{trC2}(R,S,i) := \begin{cases} F_{trCi}\left(Z_6(S,R),R,S,i\right) - F_{trCi}\left(Z_1(R,S,i),R,S,i\right) & \text{if } X(R,i) \le S \le \beta\cdot\sqrt{4\cdot i^2+R^2} \\ F_{trCi}\left(Z_6(R,S),R,S,i\right) - F_{trCi}(0,R,S,i) & \text{if } \beta\cdot\sqrt{4\cdot i^2+R^2} < S \le \beta\cdot\sqrt{1+R^2}+1 \\ 0 & \text{otherwise} \end{cases}$$

$$W_{trC}(R,S) := \left| \begin{array}{l} j \leftarrow \text{round}\left(\frac{1}{2}\cdot\sqrt{1+\frac{1}{\beta^2}+2\cdot\frac{\sqrt{1+R^2}}{\beta}}\right) \\ W \leftarrow 0 \\ \text{for } i \in -j..j \\ \quad W \leftarrow W + \begin{cases} W_{trC1}(R,S,i) & \text{if } |2\cdot i+1| \le \frac{\sqrt{1+2\cdot\beta\cdot R}}{\beta} \\ W_{trC2}(R,S,i) & \text{otherwise} \end{cases} \\ W \end{array} \right.$$

5. Transverse Radiation:

$$\Phi_{trFi}(Z,R,S,i) := \frac{2\cdot\beta\cdot R}{\left[R^2+\frac{(Z+2\cdot i)^2}{\gamma^2}\right]}\cdot\left[\frac{Z+2\cdot i}{\sqrt{R^2+(Z+2\cdot i)^2}}-\beta\right]\cdot\frac{1}{\left|\frac{1}{\beta}-\frac{Z+2\cdot i}{\sqrt{R^2+(Z+2\cdot i)^2}}\right|}$$

$$\Phi_{trBi}(Z,R,S,i) := \frac{-2\cdot\beta\cdot R}{\left[R^2+\frac{(Z-2\cdot i-1)^2}{\gamma^2}\right]}\cdot\left[\frac{Z-2\cdot i-1}{\sqrt{R^2+(Z-2\cdot i-1)^2}}-\beta\right]\cdot\frac{1}{\left|\frac{1}{\beta}-\frac{Z-2\cdot i-1}{\sqrt{R^2+(Z-2\cdot i-1)^2}}\right|}$$

$$W_{trFi}(R,S,i) := \begin{cases} \Phi_{trFi}\left(Z_1(R,S,i),R,S,i\right) & \text{if } \beta\cdot\sqrt{(2\cdot i+1)^2+R^2}-1 \le S \le \beta\cdot\sqrt{4\cdot i^2+R^2} \\ 0 & \text{otherwise} \end{cases}$$

$$W_{trBi}(R,S,i) := \begin{cases} \Phi_{trBi}\left(Z_7(R,S,i),R,S,i\right) & \text{if } \beta\cdot\sqrt{4\cdot i^2+R^2} \le S \le \beta\cdot\sqrt{(2\cdot i+1)^2+R^2} \\ 0 & \text{otherwise} \end{cases}$$

$$W_{trR}(R,S) := \left[\sum_{i=-7}^{7} W_{trFi}(R,S,i) + W_{trBi}(R,S,i)\right]$$

6. Transverse Total:

$$W_{tr}(R,S) := W_{trC}(R,S) + W_{trR}(R,S)$$

7. Normalized Longitudinal Wake Potential for a Gaussian Bunch:

$S_0 := 5$ $S_0=s_0/\sigma$ $\Sigma := 0.1918$ $\Sigma=\sigma/g$

$$W_l(R,S) := \frac{1}{\sqrt{2\cdot\pi}}\cdot\int_{-5}^{5} \exp\left[-\frac{(S-S_0-S_1)^2}{2}\right]\cdot W_{ll}(R,S_1\cdot\Sigma)\,dS_1$$

$$Ch(S) := \frac{1}{\sqrt{2\cdot\pi}}\cdot\exp\left[\frac{-(S-S_0)^2}{2}\right]$$

8. Normalized Transverse for a Gaussian Bunch:

$$W_t(R,S) := \frac{1}{\sqrt{2\cdot\pi}}\cdot\int_{-5}^{5} \exp\left[-\frac{(S-S_0-S_1)^2}{2}\right]\cdot W_{tr}(R,S_1\cdot\Sigma)\,dS_1$$